Proceedings World Geothermal Congress 2020+1
Reykjavik, Iceland, April - October 2021

Fault Characterization in Tondano Depression Using Focal Mechanism Analysis

Astha D.K Wardhani, R.M Tofan Sastranegara, Tommy Hendriansyah, Lendriadi Agung, Fadhilaz Didgaya Haq, Sigit Suryanto, and Imam B. Raharjo

Pertamina Geothermal Energy, Menara Cakrawala Lt. 19 Jalan M.H. Thamrin No. 9 Jakarta Pusat 10340

astha.dandari@pertamina.com

Keywords: focal mechanism, moment tensor, Tondano

ABSTRACT

Faults play an important role for hydrothermal fluid conduits in geothermal systems. Thus, studies of such objects are useful for geothermal exploration. One of them is seismicity. A series of faults in Tondano depression are partially covered by younger volcanic deposits, and the topographic expressions are relatively weak. This condition has become a substantial challenge when investigating the geological structures for geothermal well targetting. A focal mechanism study was conducted to identify faults geometry and to understand the faulting mechanism as well as the stress regime in Tondano depression. The study was started from the determination of major compressive and tensional stresses orientation of the region on the basis of the global earthquake database and the regional tectonic settings to the analysis of local microearthquakes focal mechanisms. Focal mechanism solutions of deep local microearthquakes events occured in Tondano depression reveal faults with two dominant strike orientations, which are SW-NE and NE-SW. The type of displacement are mostly normal right-lateral oblique and normal left-lateral oblique. This observation is in agreement with the interpretation on the fracture orientation derived from borehole fractures imaging of nearby geothermal wells which also reveals the same orientation. Relation between the major stresses orientation of the region from global earthquake dataset and local microearthquakes as well as its tectonic settings suggests that Tondano depression is extensional regime which is mainly affected by major compressional stresses from North Sulawesi Sea plate in the northwest which trends NW-SE and Molucca Sea plate collision in the east which trends E-W.

1. INTRODUCTION

Tondano depression is situated in Minahasa District where is about 40 km south of Manado city, the capital of North Sulawesi Province, Indonesia as shown in Figure 1. Geologically, it is located in Minahasa compartment which is tectonically active due to the subduction along North Sulawesi trench in the north, the movement of Tomini microplate in the south, and the double subduction of Molluca sea plate in the east. Subduction of the Molluca sea plate to the west results volcanic arc which hosts active geothermal potential in the North Sulawesi. One of geothermal fields formed due to such geological setting is Lahendong which owned and managed by Pertamina Geothermal Energy (PGE). The Unit 5 and 6 geothemal power plant of Lahendong are utilizing steam produced from wells in Tompaso area which is located within Tondano depression.

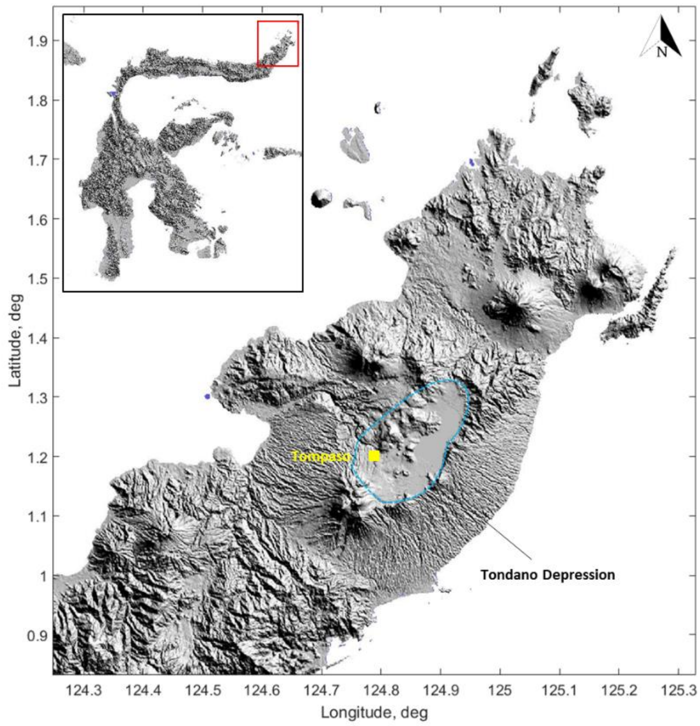

Figure 1: Location map of Tondano Depression

As the area is tectonically active region, passive seismic studies have become an effective geophysical tool to map out faulting zone. The objective of this study is to determine the faults geometry and its mechanism using microearthquakes data in Tondano depression and also to understand the relation with the major stress of regional derived from global earthquake dataset. The geometry and mechanism of fault can be determined by focal mechanism. Focal mechanism or fault plane solution provides information about the strike, dip, and rake of a fault as well as the orientation of the major compressive and tensional stresses, thus tectonic deformation of the region can be estimated.

2. REGIONAL BACKGROUND OF TONDANO DEPRESSION

2.1 The Volcano Tectonic Settings of North Sulawesi

Tondano depression lies within the Sangihe volcanic arc in the Minahasa compartment in the northeastern sector of Sulawesi Island (Figure 2). The volcanic arc is believed to have been formed by the subduction of the Molucca sea plate resulting from the collision of Sangihe and Halmahera forearcs (Hamilton, 1979). The fault structures in Minahasa compartment resulted from the movement of Sulawesi Sea plate from the north and the micro-plate of Tomini from the south (Siahaan et al., 2005). The effect of the two stresses from north and south, the north arm of Sulawesi plate moved eastward that collides with westward movement of Moluccas oceanic plate. Tondano is considered as a volcano tectonic depression.

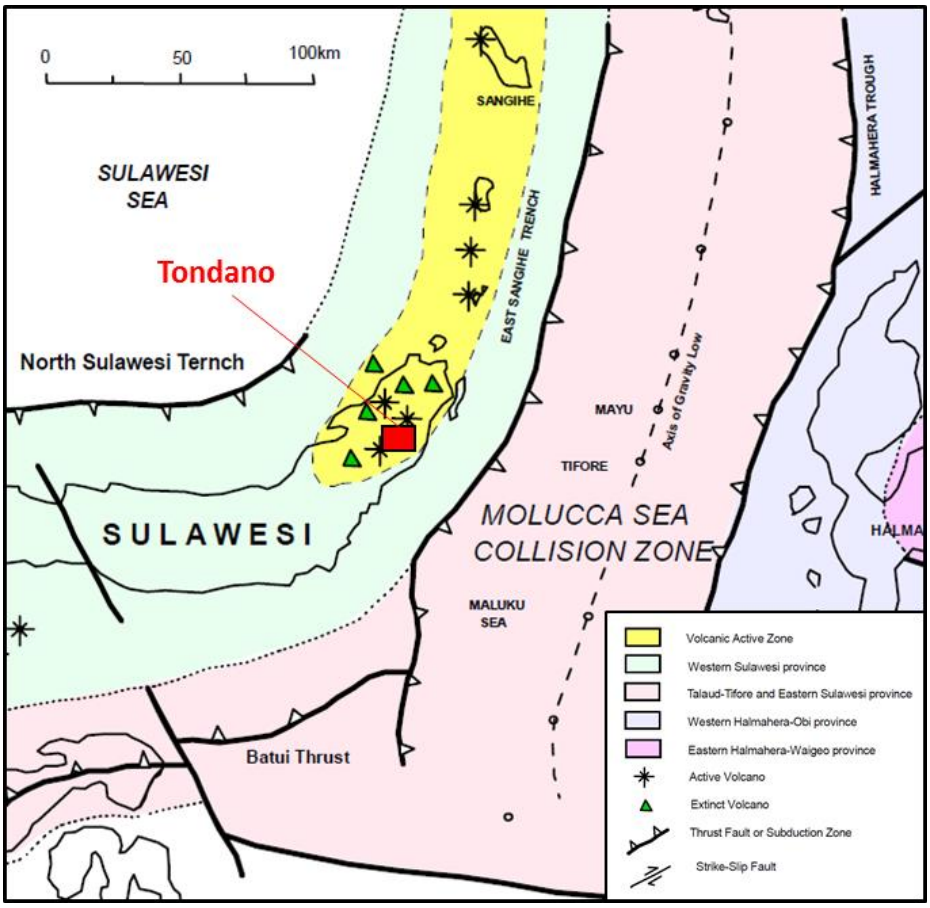

Figure 2: Regional tectonic setting of North Sulawesi (Siahaan, 2005 modified from Hamilton, 1979; Sukamto, 1989)

2.2 Focal Mechanism of North Sulawesi and The Surroundings

The study was started from mapping focal mechanism solution of global earthquakes data set downloaded from Global Centroid-Moment-Tensor (CMT) Project catalogue, formerly known as Harvard-CMT (Dziewonski et al., 1981). This project routinely determines focal mechanism by moment tensor inversion of an earthquake. Earthquakes dataset of North Sulawesi and the surroundings were used in this study. The filter criteria for the earthquakes were defined by latitude of -0.02° S to 2.20° N and longitude of 123.03° E to 126.34° E, time period of March 29th 1977 to December 31th 2018, magnitude of 0 – 10, and depth 0 – 1000 km.

There are 327 earthquakes focal mechanism data observed for such criteria. The magnitudes of earthquakes ranged from 4.8 to 7.6, located at depth 13 to 284 km. The result reveals three earthquake populations as depicted in Figure 4 with the following interpretations:

1) Earthquakes located in North Sulawesi Sea at depth ranged from 15 to 284 km are associated with active tectonic defomation of south-dipping Sulawesi subduction plate. It is represented by focal mechanism which mostly shows thrust faults with E-W strike orientation, parallel to the North Sulawesi trench axis.

2) Earthquakes located in south of the North Sulawesi at depth ranged from 25 to 267 km are related to active movement of Tomini microplate. The focal mechanism shows thrust faults with more various strike orientations but mostly NE-SW.

3) Earthquakes located in northern Molucca Sea at depth ranged from 13 to 167 km are correlated with Molucca Sea plate collision activities. It is reprsented by focal mechanism which shows mostly thrust fault with S-N strike orientation, parallel to the Sangihe and Halmahera trench axis.

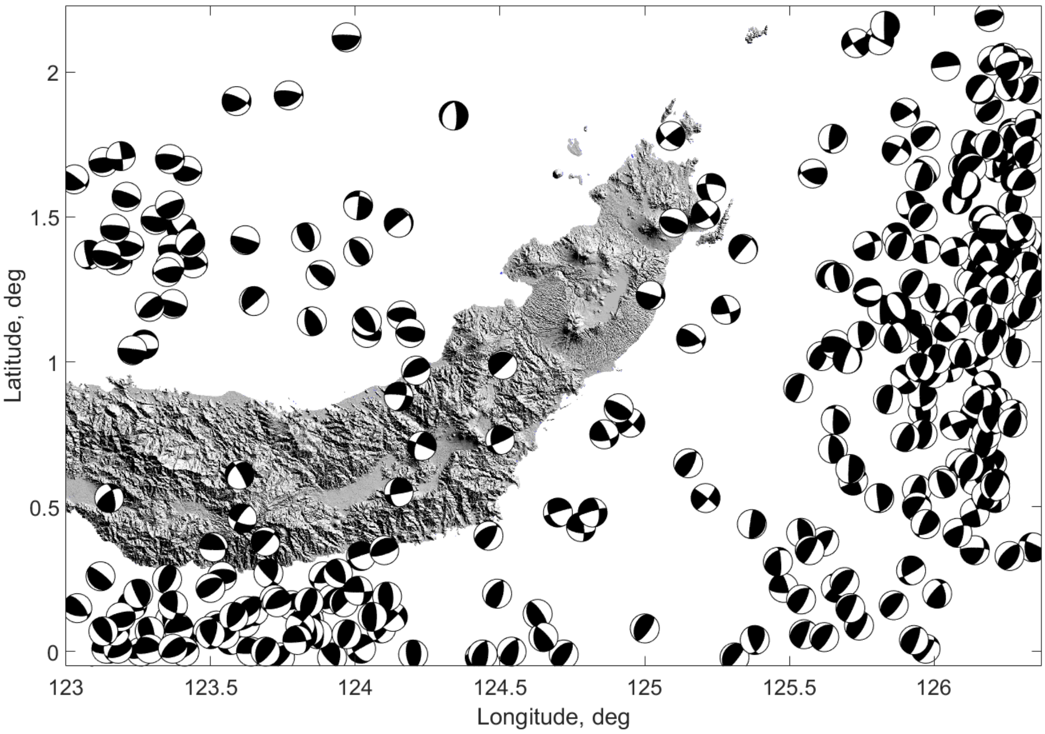

Figure 3: Focal mechanism of North Sulawesi and the surroundings from Global CMT catalogue. Black and white symbol is fault plane solution with black corresponds to compressional field and white corresponds to dilatational field.

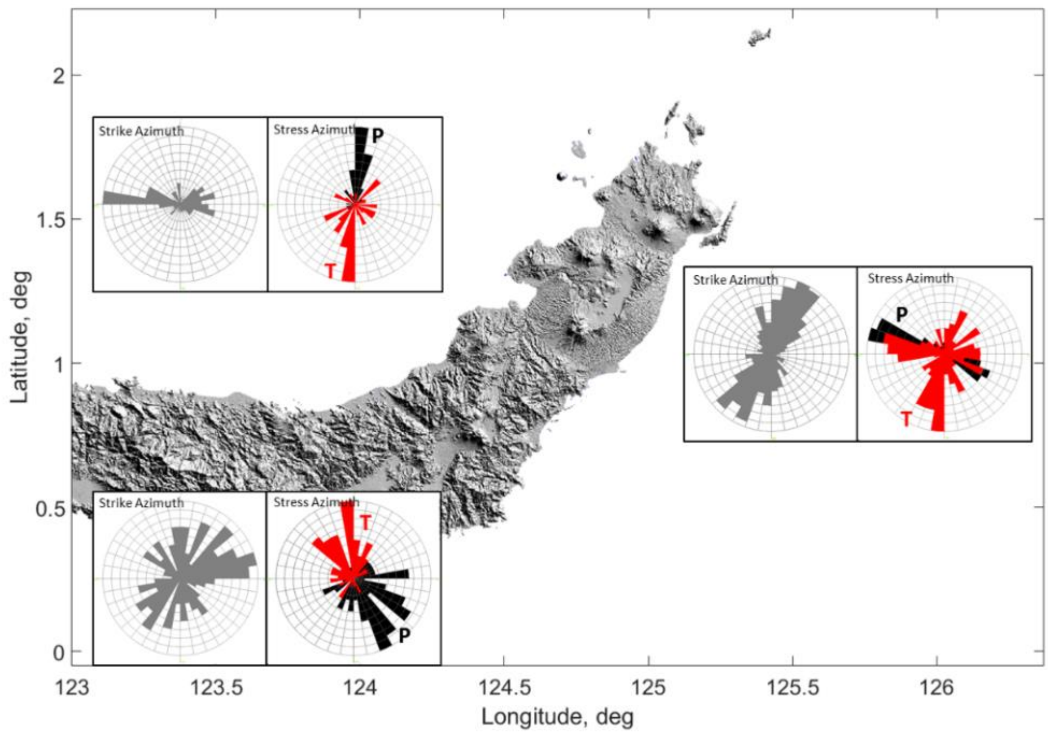

Figure 4: Fault plane strike and major stress orientation of North Sulawesi and surroundings. The maximum compressional stress (P) axis direction is horizontal and the maximum tensional stress (T) axis direction is vertical.

The directions of maximum amplitudes in the compressional (shaded as black) and dilatational (unshaded) fields define the pressure (P) and tension (T) axes. P and T imply “compression” and “tension”, respectively, the stress condition before faulting

(Lowri, 2007). The P-axis often coincides with the axis of maximum compressional stress (σ_3) which also corresponds to the axis of minimum tensional stress in dilatational field. The T-axis is often equated with the axis of maximum tensional stress (σ_1) which corresponds to the axis of minimum compressional stress in compressional field. However, the P and T axes actually indicate principal shortening and lengthening (strain) directions which may deviate significantly from the principal stress axes σ_3 and σ_1 (Gephart, 1986). The magnitudes of principal stresses are defined by $\sigma_1 > \sigma_2 > \sigma_3$. Figure 4 shows the P and T axes orientations derived from Global CMT for three different earthquake populations in North Sulawesi and surroundings.

The type of displacement of all earthquakes is almost entirely reverse, associated with subduction activities in the north, south, and east of North Sulawesi. It implies that P-axis direction is horizontal and the T-axis direction is vertical. The P-axis azimuth orientations of North Sulawesi Sea earthquakes are dominantly N 0° to 20° E or nearly oriented to N-S which are parallel with the subduction direction to the south. The T-axis azimuth orientations are mostly N 180° to 200° E. The P and T-axis azimuth orientations of earthquakes located in south of the North Sulawesi are more various which are within N 90° to 180° E or oriented to SE-NW while the T-axis azimuth orientations are within N 270° to 360° E. The P-axis azimuth orientations of northern Molucca Sea earthquakes are mostly N 280° to 300° E (W-E) and N 110° to 130° E (E-W) which are parallel with the direction of Molucca Sea plate collision. The T-axis azimuth orientations are more various, mostly N 180° to 210° E and N 270° to 290° E.

2.3 Geological Settings of Tondano Depression

The formation of Tondano depression occured during major eruptive episodes of old volcano related to Sangihe arc volcanism, resulting 20 x 10 km diameter caldera open to west (Lecuyer et al, 1997). It is characterized by the wide spread deposition of pyroclastic rocks composed of tuff, lapilli and ignimbrite (Siahaan et al, 2015). The major eruptive episodes were followed by the Quarternary volcanic activites which occured at the Lahendong complex in the central, Sempu-Soputan complex in the south and Lokon-Empung complex in the north Tondano Caldera (Sardiyanto et al, 2015). Several eruptions still occur at present which the most intensive volcanic activities are located in Lokon-Empung, Soputan, and Mahawu.

In the southern part of Tondano depression, a series of NE-SW and SW-NE trending faults comprise the dominant orientation in the area, while the major structure is ENE-WSW trending fault which cuts Rindengan slope to Tempang as shown in Figure 5. Some parts of the faults are partially covered by younger volcanic deposits so that the topographic expressions are slightly limited. The ENE-WSW trending fault is proposed as hydrothermal fluid conduits in Tompaso geothermal system.

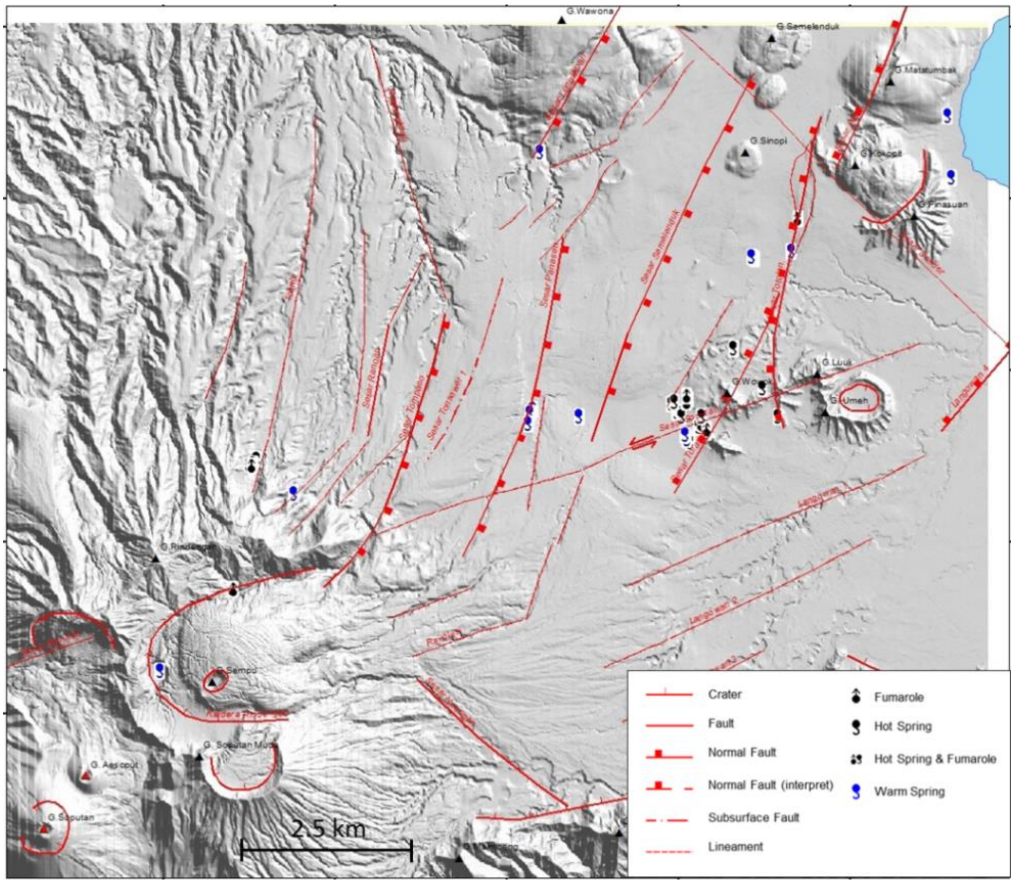

Figure 5: Geologic structure map of Tompaso (PGE, 2018)

3. FAULT CHARACTERIZATION IN TONDANO DEPRESSION

3.1 Microaerthquakes Focal Mechanism Data and Processing

The faults geometry and mechanisms in Tondano depression were determined using focal mechanism of microearthquakes data recorded by 14 geophones which has been deployed in Lahendong-Tompaso geothermal field. Seismic stations network is illustrated in Figure 6. The acquisition utilized 3-triaxial components geophone with 4.5 Hz natural frequency. Sampling rate was set to 200 hertz.

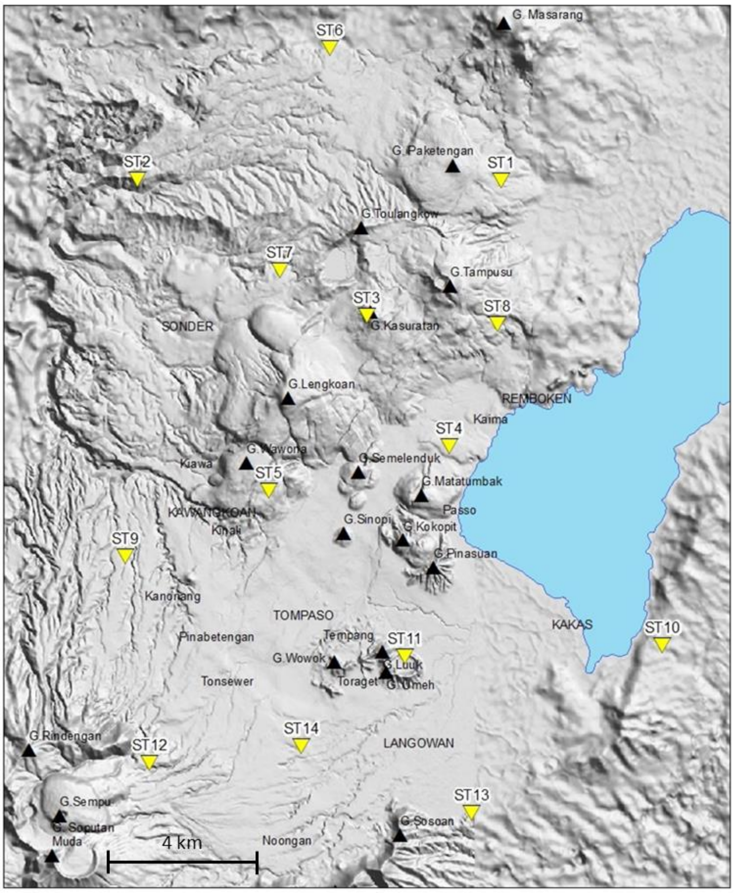

Figure 6: Seismic station network. Stations are shown as yellow triangle.

Earthquake events were automatically detected using the automatic picking routine based in the SAPS seismological data acquisition and processing system that utilized in the SMARTQuake® program (Oncescu, M.C., et al., 1996). Regional events were not further proccesed due to the limitation of stations network coverage, thus only local events were selected to be analysed. In this study, local event was roughly defined by arrival time difference between S and P-waves is less than 3 seconds. Due to this criteria, 148 local microearthquakes events were obtained.

Hypocenter determination was started from picking the P and S-waves first arrival times manually using interactive SEISPLUS program, then computed them using robust location program called HYPOPLUS which is also utilized in the SEISPLUS (Oncescu, M.C. and Rizescu, M., 1997). This program applies Geiger iterative method. The P-waves first motion polarity picking is required for the focal mechanism determination.

A number of microearthquake events with depth of 4 – 10 km and magnitude range of -0.1 – 2.4 were observed in Tondano depression. High signal to noise ratio (S/N) of seismograms of some events cause the certainty of first arrival time picking increased, as a result some events have quite low hypocenter location errors, which is averagely 0. 5 km for horizontal position and 0.7 km for depth. The other events have quite high hypocenter location errors which is about 1 km for horizontal position and 1.2 km for depth due to poor quality seismograms that cause errors in first arrival time picking. The error of hypocenter determination is also affected by inadequate velocity model used in the processing.

The faulting mechanism was studied using focal mechanism moment tensor inversion for each microearthquake data. Moment tensor inversion was performed using SEISPLUS program. The program performs moment tensor inversion for local earthquakes based on spectral amplitudes of body wave trains, following a method developed by Ebel and Bonjer (1990) and automated by Rizescu (1999). The calculation requires hypocenter information, polarity of P-wave first motions (up or down), and amplitudes. The output includes strike, dip, rake of two nodal planes, P, B, T-axis azimuth with its plunge, and a stereographic projection on the lower focal hemisphere. Several data could not be computed due to either poor quality or event location outside the station network, causing number of focal mechanism reduced to 51 events.

3.2 Interpretation on Focal Mechanism of Tondano Depression

Focal mechanism solutions of microearthquake events occured in Tondano depression are depicted in Figure 7. Each solution gives two nodal planes, one being the fault plane and other being the auxilliary plane. Due to such ambiguity, other data was used to decide which nodal plane is the active fault plane. This study used geological structure and lineament map as demonstrated by previous studies as well a recent investigation of borehole fracture imaging from geothermal wells to determine the active fault plane. Focal mechanism solution reveals two dominant strike orientations, which are SW-NE and NE-SW trending with dip mostly ranged from 50° to 90° as presented in Figure 8. The result shows similarity of fault orientations demonstrated by Sardiyanto (2015) in the geological structure modeling of Tompaso geothermal field constructed from geological mapping, satellite images interpretation and borehole images log. The rake angle indicates the type of displacement of the faults, which are mostly normal right-lateral (dextral) and left-lateral (sinistral) oblique-slip.

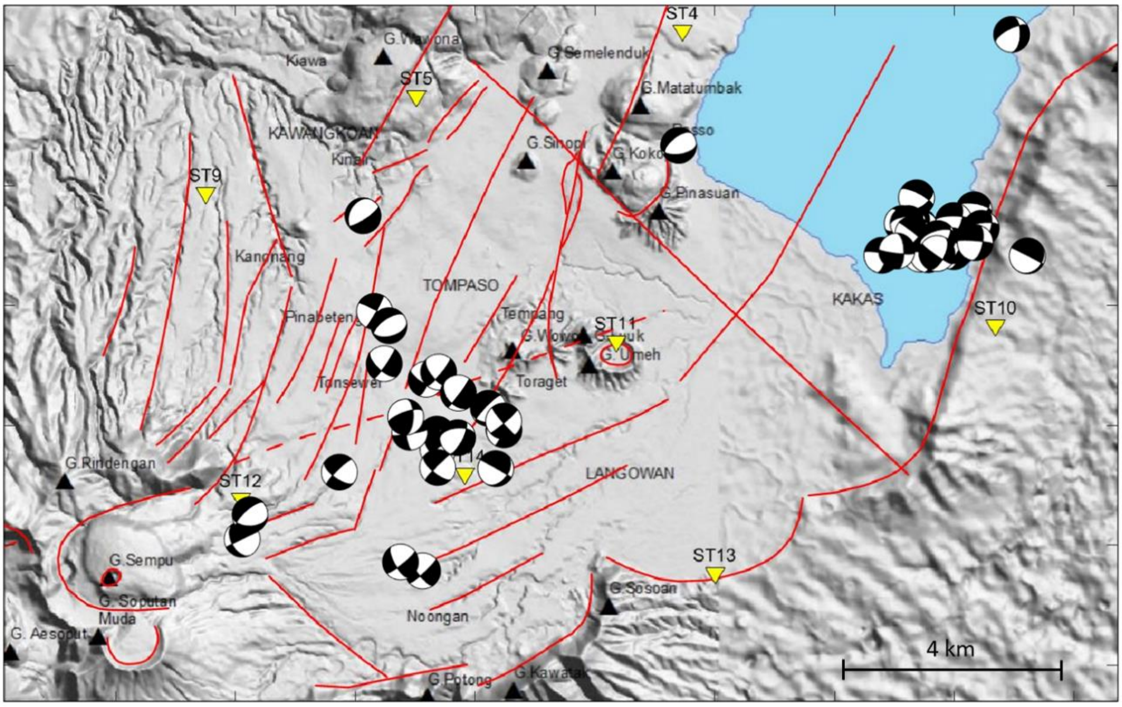

Figure 7: Focal mechanism map of Tondano depression. Black and white symbol is the fault plane solution, black corresponds to compressional field and white corresponds to dilatational field; yellow triangle is seismic station.

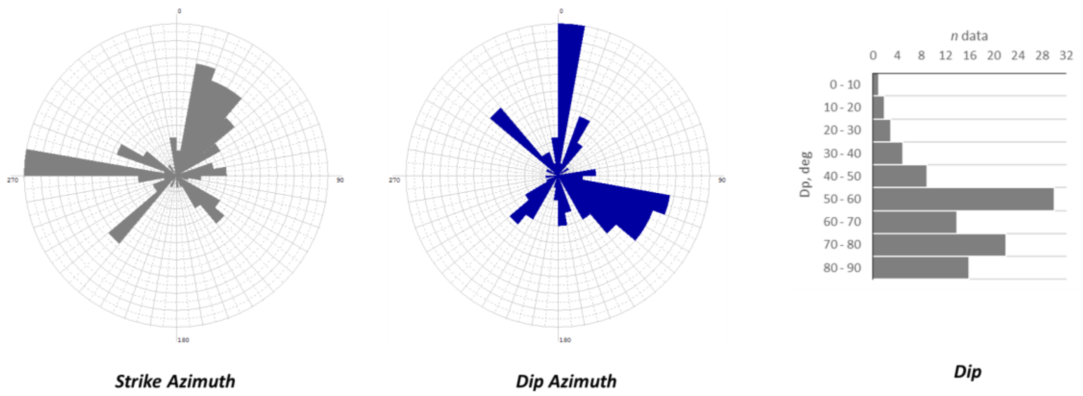

Figure 8: Rose diagram of strike azimuth (left) and dip azimuth (center), as well as dip angle histogram (right) of possible fault-planes in Tondano depression revealed from focal mechanism.

Microearthquakes focal mechanisms were classified into 3 groups according to similarity on the major maximum compressive and tensional stresses P and T-axes azimuth orientations. The first group is the ones with P-axis azimuths that trend E-W and T-axis azimuths that trend N-S. This state of stresses could form two possible faults as depicted in Figure 9, one trending N 224°– 243° E or SW-NE orientation, dipping 63° – 90° to northwest, having rake angle of 210° – 257°, and the other trending N 88°– 153° E or SE-NW orientation, dipping 20° – 60° to southwest, having rake angle of 305° – 359°. The recent investigation of borehole conductive fractures orientation from nearby geothermal well LHD-40 identified the conductive fractures (presumed open) with dominantly SW-NE strike orientation dipping to west as shown in Figure 10. Knowing such information, the active fault plane can be confidently associated with the plane trending SW-NE with normal right-handed (dextral) oblique-slip movement. The topographic lineament also supports this observation. The normal oblique movement indicates that the maximum tensional stress σ_1 direction is horizontal, while the minimum tensional stress σ_3 direction is vertical.

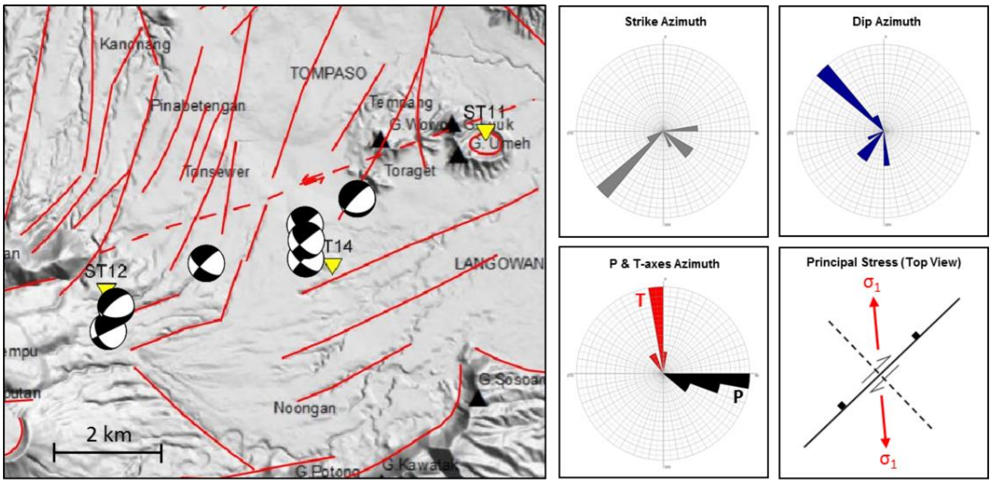

Figure 9: SW-NE dextral oblique-slip normal faulting mechanism in Tondano depression and its P and T-axes orientations. The σ1 direction is horizontal and the σ3 direction is vertical.

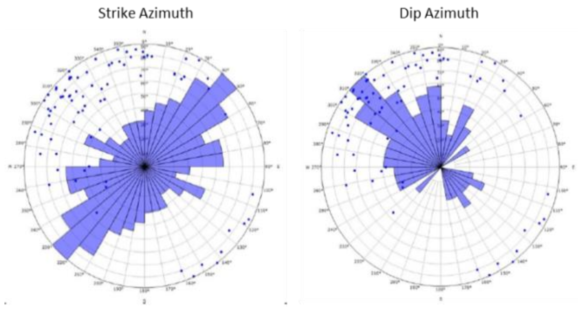

Figure 10: Strike orientation and dip azimuth of conductive fracture from well LHD-40 (PGE, 2014).

The second group is the ones with P-axis azimuths that trend NNW – SSW and T-axis azimuths that trend E – W as presented in Figure 11. In such condition, two possible faults could be formed as presented in Figure 11, one trending N 110°– 140° E or SE-NW orientation, dipping 52° – 69° to south, having rake angle of 192° – 221°, and the other trending N 2°– 40° E or NE-SW orientation, dipping 52° – 83° to southeast, having rake angle of 229° – 335°. The NE-SW trending fault plane is suggested as the active fault plane which is roughly aligned with borehole major conductive fractures orientation of well LHD-27 which shows mostly NE-SW orientation dipping to southeast as shown in Figure 12. The type of fault displacement is normal left-handed (sinistral) oblique-slip movement which also indicates that the maximum tensional stress σ_1 direction is horizontal, while the minimum tensional stress σ_3 direction is vertical.

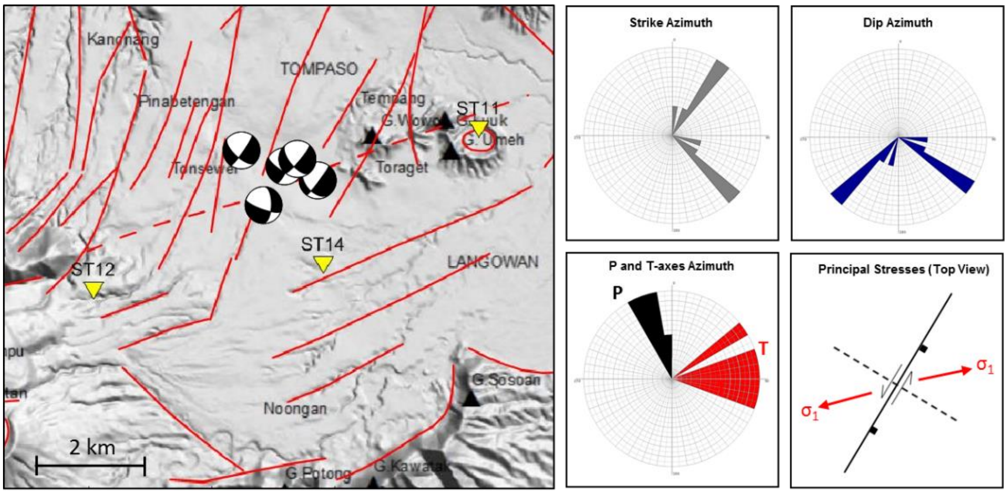

Figure 11: NE-SW sinistral oblique-slip normal faulting mechanism in Tondano depression and its P and T-axes orientations. The σ1 direction is horizontal and the σ3 direction is vertical.

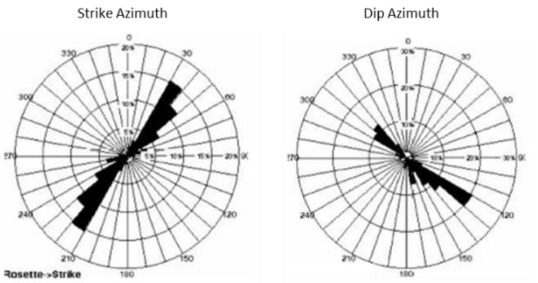

Figure 12: Strike orientation and dip azimuth of conductive fracture from well LHD-27 (PGE, 2009).

The third group is the ones with P-axis azimuths that trend SW – NE direction and T-axis azimuths that trend NW – SE. The events were occurred sequentially within a day, situated at 8 – 10 km beneath the southernmost of Tondano Lake which might be related to tectonic deformation activities in this area. The fault-plane could be either trending N 10° – 20° E, dipping 53° –66° to northeast, having rake angle of 188° – 240°, or trending N 270° – 280° E, dipping 59° – 80° to north, and having rake angle of 280° – 335° as depicted in Figure 13. The active fault-plane could not be decided due to the lack of supporting data in this area. Nevertheless, both of the fault displacements are also discovered as normal oblique which suggests that the maximum tensional stress σ_1 direction is horizontal, while the minimum tensional stress σ_3 direction is vertical.

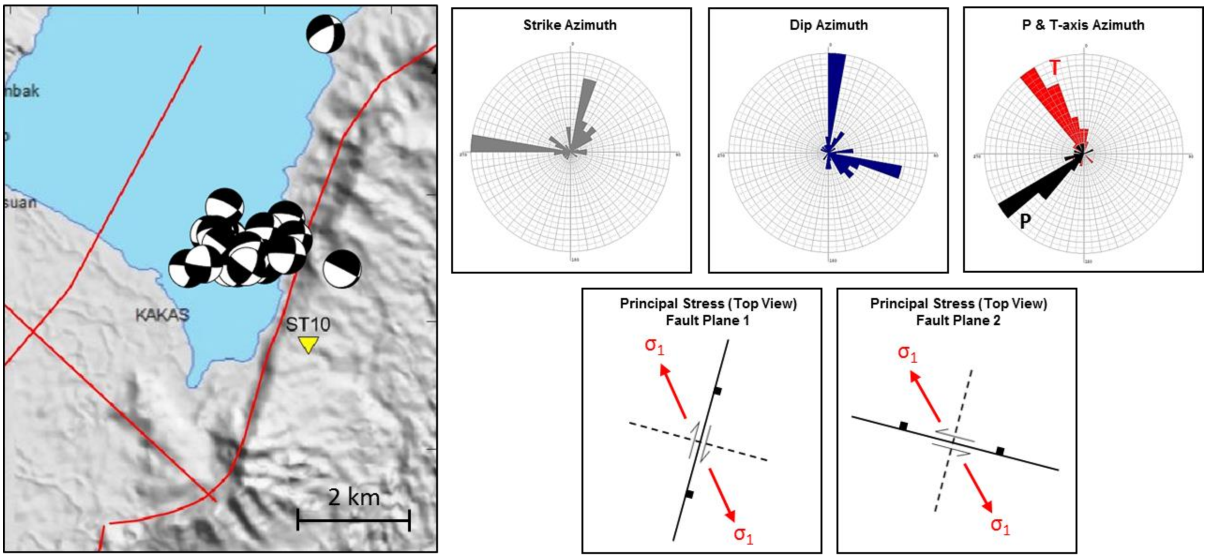

Figure 13: Possible faulting mechanisms in Tondano depression striking either NNE-SSW or W-E with its P and T-axes orientations. The fault displacement could be normal dextral oblique or normal sinistral oblique. The σ1 direction is horizontal and the σ3 direction is vertical.

The stress regime in Tondano depression is mainly affected by major compressional stresses from North Sulawesi Sea plate in the northwest that trends NW-SE (relative to Tondano depression area) and Molucca Sea plate collision in the east that trends almost E-W. Focal mechanism of the microearthquakes indicates extensional regime which is characterized by oblique-slip normal faulting, expressing stress release of two major maximum compressional stresses in the northwest and east of the region.

4. CONCLUSION

The focal mechanism analysis has successfully demonstrated the faulting mechanism in Tondano depression, which are characterized by SW-NE and NE-SW trending fault with normal dextral and sinistral movement. This observation is in agreement with the topographic lineament as well as the major conductive fracture orientations from borehole data of geothermal wells which also trend to the same orientation. The whole fault displacements are oblique-slip normal with either sinistral or dextral movement, indicating that the region is extensional regime. Relation between the major stresses orientation of the region from global earthquake dataset and local microearthquakes as well as its tectonic settings suggests that the faults deformations in Tondano depression are strongly affected by major compressional stresses from North Sulawesi Sea plate in the northwest that trends NW-SE and Molucca Sea plate collision in the east that trends E-W.

REFERENCES

Dziewonski, A.M., Chou, T.A. and Woodhouse, J.H.: Determination of Earthquake Source Parameters From Waveform Data For Studies of Global and Regional Seismicity: Journal Geophysics Research, v. 86, (1981), 2825-2852.

Ebel, J.E., and Bonjer, K.P.: Moment Tensor Inversion of Small Earthquakes in Southwestern Germany for the Fault Plane Solution: Geophysical Journal International, Vol. 101, (1990), 133-146.

Ekström, G., Nettles, M., and Dziewonski, A.M.: The global CMT project 2004-2010: Centroid-moment tensors for 13,017 earthquakes, Phys. Earth Planet. Inter., 200-201, 1-9, 2012. doi:10.1016/j.pepi.2012.04.002

Gephart, J.W.: Principal Stress Directions and The Ambiguity in Fault Plane Identification From Focal Mechanisms: Bulletin of The Seismological Society of America, Vol 78, (1986), 621-625.

Hamilton, W.B.: Tectonic of The Indonesian Region: United States Geological Survey (1979).

Lecuyer, F., Bellier O., Gorgaud A., Vincent P.M.: Active Tectonics of Northeast Sulawesi (Indonesia) and Structural Control of The Tondano Caldera, Earth & Planetary Sience, Vol. 325, (1997), 607-613.

Lowrie, W.: Fundamentals of Geophysics (2nd edition): Cambridge University Press, New York (2007).

Oncescu, M.C., and Rizescu, M.: SAPS v3.0 – Seismological Acquisition and Processing System, User's Guide, Karlsruhe, (1997), 82.

Oncescu, M.C., Rizescu, M. and Bonjer, K.P.: SAPS – A Completely automated and networked seismological acquisition and Processing System, Computer & Geoscience, 22, (1996), 89-97.

Pertamina Geothermal Energy: Fracture Study of Well LHD-27 based on Borehole Resistivity Imaging: Pertamina Geothermal Energy Internal Report (2009).

Pertamina Geothermal Energy: Fracture Study of Well LHD-40 based on Borehole Resistivity Imaging: Pertamina Geothermal Energy Internal Report (2014).

Pertamina Geothermal Energy: Geological Structure of Tompaso: Pertamina Geothermal Energy Internal Report (2018).

Rizescu, M.: A Completely Automated System For Seismological Data Acquisition, Processing and Exchange: PhD Thesis, Institute for Atomic Physics, Bucuresti, (1999), 219.

Sardiyanto, Nurseto, S.T., Prasetyo, I.M., Thamrin, M.H., and Kamah, M.Y. Permeability Control on Tompaso Geothermal Field and Its Relationship to Regional Tectonic Setting: Proceeding World Geothermal Congress 2015, Melbourne, Australia (2015).

Siahaan, E.E., Soemarinda, S., Fauzi, A., Silitonga, T., Azimudin, T., and Raharjo, I.B.: Tectonism and Volcanism Study in The Minahasa Compartment of North Arm of Sulawesi Related to Lahendong Geothermal Field, Indonesia: Proceeding World Geothermal Congress 2005, Antalya, Turkey (2005).

Sukamto, R.: Halmahera, A Typical Cainozoic Volcanic Island Arc in Eastern Indonesia: Journal of the Indonesian Association of Geologists, Vol. 12, (1989), 1.